Correction: Statistics and structure of turbulence in a fan/FEGV interstage and their aeroacoustic implications

Sheryl Grace * and Ankush Gupta †
Dept. of Mechanical Engineering
Boston University, Boston, MA 02215

Ignacio Gonzalez-Martino ‡
Aerospace Application Management, Exa Corporation, Paris, France

Damiano Casalino, §
Dept. of Aerodynamics, Wind Energy, Flight Performance and Propulsion
Delft University of Technology, 2629 HS Delft, The Netherlands

Modern computational capabilities make simulations of complicated flow fields such as those in the fan stage of a turbofan engine possible. In particular, time resolved simulations are presenting new opportunities for studying the disturbances responsible for the broadband noise created by the fan stage. A preliminary quantitative analysis of the simulated flow field in the gap between the fan and fan exit guide vane (FEGV) computed with the Lattice Boltzmann based software PowerFLOW is presented. The study compares the simulated flow with experimental measurements to assess the mean flow, the turbulence intensity, the turbulence length scale and the turbulence dissipation rate. The mean wake is shown to be more diffuse than measured experimentally and the turbulence length scale of the simulated data is 1.5 times greater than that deduced from the measurements while the simulation based dissipation rate is slightly less than the measurement based value. The overprediction of the length scale is shown to potentially have a significant effect on the broadband noise. It is hypothesized that the overprediction is due to the usage of a trip to trigger the turbulent transition on the rotor blade in the computation. This preliminary study provides a path for more detailed wake evolution analysis using the simulation data as well as further flow comparisons for different stage configurations and fan operating speeds.

I. Introduction

Interaction noise due to rotor wake flow through a fan exit guide vane (FEGV) in the fan stage of a turbofan engine leads to both tonal and broadband noise. The prediction of the noise from the fan stage continues to be of interest as fan noise is now a key engine noise source. Of interest in this paper is the prediction of the broadband noise. Many simulation methods have been proposed for predicting the broadband noise. Some that focus on the dominant interaction noise utilize a two-step approach in which the wake turbulence is modeled or obtained via experiment as a first step and then the interaction of the turbulence with the FEGV

*Associate Professor, AIAA Associate Fellow
†Graduate Student
‡AIAA Member.
§Professor, AIAA Member

is considered as a second step. Such predictions are dependent on accurate fan wake turbulence quantities. Another approach is to more directly compute the acoustics by resolving the acoustic pressure at the inlet and/or exhaust planes. Multiple noise sources would be captured using the direct method and the turbulence must be well modeled for this method to work.

The Source Diagnostic Test (SDT) performed by NASA in the late 90s has provided a benchmarking platform for simulations of fan noise.[1,2,3,4] For the lowest fan speeds tested, hotwire data were obtained upstream of the FEGV. These data were explored in Ref. [5] to determine the turbulent characteristics of the rotational flow generated by a turbofan. The turbulence intensities were shown to be reasonably approximated with an isotropic relation and the turbulent kinetic energy was shown to be fairly well predicted by Reynolds Averaged Navier Stokes (RANS). The dissipation rate computed from the experimental data using structure functions does not agree in magnitude with the ϵ values from RANS but does have the same trend from hub-to-tip. The streamwise longitudinal length scale was shown to agree reasonably well with the length scale one can obtain from the heuristic based combination of k and ϵ values from RANS.

The hotwire data can be used directly in the two-step noise calculation. However, only the lowest rotor speed can be computed this way. For the higher rotor speeds, where hotwire data were unobtainable, the inflow to the vanes must be derived another way. Computations make sense for filling this gap. Another caveat associated with the hotwire velocity data (also true for RANS based flow data) is that only the streamwise longitudinal length scale can be calculated from the data. In most of the two-step methods, both the streamwise longitudinal and the radial transverse length scales play a role. Hence, up to now, the radial length scale has simply been estimated.

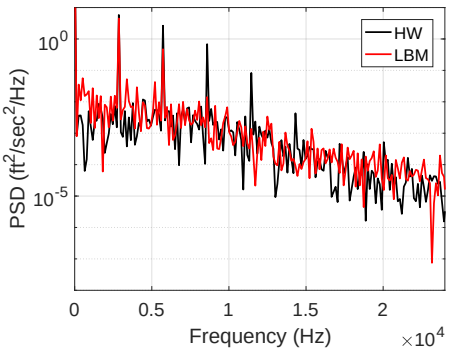

Figure 1: Example comparison between measurement and computational data. Axial flow velocity spectrum.

Recently, large eddy simulation (LES)[6] and very large eddy simulation methods (VLES)[7] have been used to resolve the fan stage flow field. In fact, the Lattice Boltzman Method (LBM) implemented in the PowerFLOW code developed by EXA has been used to perform full turbulent simulations of the SDT and related cases.[7] Because PowerFLOW uses a VLES, the velocity time traces can be analyzed exactly as the hotwire data are analyzed. It is of interest to explore whether the EXA VLES method reproduces the flow field accurately. Qualitative assessments of the mean velocity and turbulent kinetic energy color contours at axial slices in the gap have shown good agreement. As well, the power spectral density (PSD) obtained from an FFT of the data provide some confidence that the simulations capture important features in the gap flow. For instance, Figure 1 shows the comparison between the PSD of the axial flow at the midgap, midspan location for one of the fan simulations performed previously using PowerFLOW. It is argued that both the tonal and broadband nature of the flow field are reasonably well predicted by the simulation. The statement does seem true from the figure; but, it is only a qualitative comparison.

This paper analyzes the mean and turbulent flow quantities computed with PowerFLOW following the quantitative method described previously in Ref. [5] and utilized in Refs. [8,9]. Circumferentially averaged and overall mean values of the background velocity are analyzed. The turbulence intensity, length scales and dissipation rate are all considered. The EXA simulations related to the SDT encompass 10 rotor revolutions while the HW data encompass more than 100 rotor revolutions. The effect of utilizing only 10 revolutions is shown in this paper to be inconsequential. Finally, the PowerFLOW data are used as input to a low-order

broadband acoustic calculation method in order to draw conclusions concerning the effect of differences in the simulated and measured data on an acoustic prediction.

The paper is organized in the following way. First, the SDT configuration used in this paper will be described as well as EXA's computational set-up of the problem. The method for analyzing the data is described in the Method section. The comparison of the relevant turbulent quantities between the PowerFLOW simulations and the hotwire data are then shown. Finally, the difference in the broadband prediction based on whether the input is derived from hotwire or simulation data are shown.

II. SDT configuration and computational setup

Fig. 2 illustrates SDT fan rig with the the Low-Noise vane. The geometry is perfectly axisymmetric. The rotor radius is 10.97 in, the bypass exhaust radius is 10.66 in and the lip intake radius is 11.66 in.The rotor consists of 22 blades with a casing/blade-tip gap of about 0.02 in. The Low-Noise vane has 26 swept vanes. The other two vane geometries that were tested were unswept and included a low count and a baseline case. The low-count case has 26 vanes similar to the low-noise vane. The baseline case has 54 smaller vanes. At the approach rotor speed both hotwire and laser-doppler velocimetry (LDV) data were acquired. The measurements were taken at two axial locations referred to as stations 1 and 2 throughout this paper. The first station was placed midway between the rotor and exit guide vane and the second station was at a location very near where the leading edge of the unswept vane cases which is why the data were acquired using the swept vane. 50 radial locations were used for hotwire measurement. LDV data were acquired at 44 radial positions at station 1 and 45 positions at station 2. The flow data were originally described and analyzed in Ref. [10].

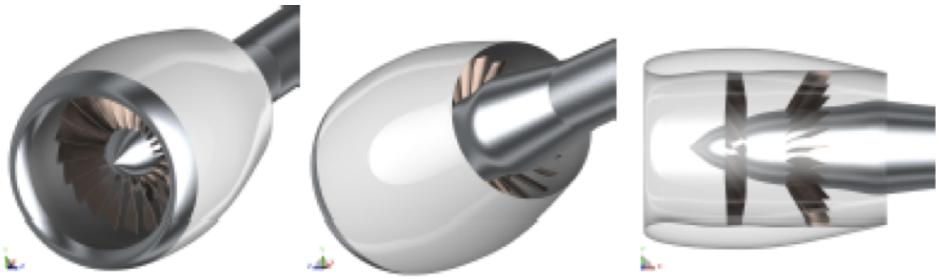

Figure 2: Reference SDT Low-Noise configuration.

In the present work, computational data from a simulation related to the baseline vane SDT case at the approach rotor speed is analyzed. Figure 3 shows a wavy leading edge modification for which the calculations were performed. Details of the computational setup, some turbulent flow analysis, and far-field acoustic results obtained using a Ffowcs-Williams and Hawkings approach within the PowerFLOW software have been given previously.[11] The approach fan speed of 7808 RPM is the focus of this study. The gap-flow analysis in this paper uses data from the volume shown in red in Figure 3.

All simulations reported in this paper have been performed by using, as initial condition, the solution obtained by using a coarser mesh and achieving an acceptable statistical convergence. The time step is 2.183×10^{-6} s and the simulations are performed by sampling the solution along 10 rotor revolutions after a very short initial transient of three blade passages. The CPU cost is of the order of six thousand CPU hours per rotor revolution using 720 cores Intel Sandybridge 2.7 GHz.

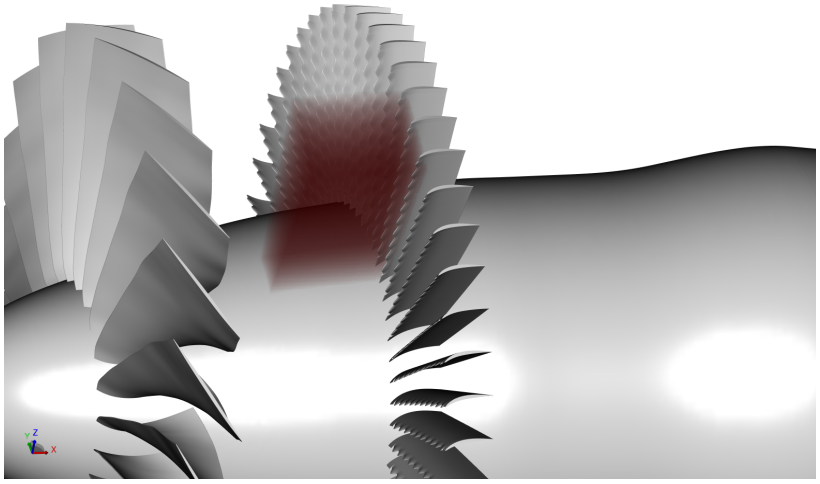

Figure 3: Geometry used in PowerFLOW simulation and volume from which data were extracted and analyzed.

III. Method

Throughout this paper, the flow coordinate system that will be used is labeled streamwise, upwash, and radial. Once the radial flow direction is set, the other two directions are determined by calculating the overall mean flow angle at a given location. The mean flow angle sets the streamwise direction and the upwash direction is perpendicular to the streamwise direction. This is slightly different from the frame of reference described by Podboy[10] where the radial flow was not separated first. In order to easily compare the current results with those in Refs. [10, 8, 9] the Imperial Unit system is used throughout this paper.

A. Mean flow

To analyze the mean flow both circumferentially averaged and total mean flow views of the flow field at stations 1 and 2 are considered. When the circumferentially averaged values are plotted, the minimum flow point for the streamwise flow is aligned with the center of the passage at the midspan location. The same shift is then used for subsequent span locations and for the other flow components. While the streamwise and upwash flow directions are most often used in this analysis, the mean flow is also projected into the axial and circumferential directions so that the current results can be easily compared to past analyses.

B. Turbulent flow

The gap flow quantities that have been analyzed previously because they are used as input to the low-order vane response calculation include the turbulence intensity and the integral length scale. Because these quantities may be based on computational fluid dynamic simulations, the turbulent kinetic energy and the the turbulent dissipation have also been studied in order to probe the validity of k and ϵ quantities used in a Reynolds Averaged Navier Stokes turbulence model. In this work, the turbulence intensity, RMS velocity, is obtained from both the hotwire data and the LBM results by first performing an FFT on the time resolved velocity data. The DC offset and first four tones are removed from the FFT result. An inverse FFT is then performed to obtain the turbulent part of the velocity signal. The turbulent signal is then squared, averaged, and then the square root is taken to obtain an RMS value. The total RMS value at a radial probe location

is obtained as well as the circumferentially averaged values. Again, if an average passage value is reported, the peak value of the streamwise component is shifted to the midpassage location at midspan and all other components and spanwise results are shifted by the same amount. RMS values measured with the LDV have been distributed by NASA. Differences between the supplied LDV RMS values and those computed from the hotwire data will be discussed in the results section.

The integral length scale is of interest for broadband vane response calculations because the turbulent flow in the gap approaching the vane is represented by its spectrum. The Leipmann spectrum is often used which states

$$E_{u,u}(\mathbf{k},t) = (2\pi)^3 \frac{2u_u'^2}{\pi^2} \frac{L_s^5(k_s^2+k_r^2)}{(1+(kL_s)^2)^3} \tag{1}$$

with L_s denoting the longitudinal streamwise integral length scale and $k = \sqrt{k_s^2+k_u^2+k_r^2}$. The subscripts refer to streamwise, upwash, and radial directions. The spectrum of interest is noted here as the upwash spectrum because it is assumed that the streamwise flow is alligned with the vane and thus the upwash flow produces the unsteady forcing of the vane. Taylor's frozen turbulence hypothesis is assumed such that the convection of the turbulence can be taken to be entirely due to the mean flow. Hence the flow probes (either physical hotwire or computational data retrievals) will measure the local flow with $x_s = U_s t$ where x_s is distance in the streamwise direction. (It is noted again that streamwise here is not comprised of any of the flow in the radial direction.) The streamwise length scales, both longitudinal and transverse, can be obtained then from the time series data as

$$L_{s_i} = \overline{U_s} \int_0^\infty \frac{\overline{u_i'(\tau)u_i'(\tau+t)}}{u_i'^2} dt \tag{2}$$

where i becomes s for streamwise, u for upwash, and r for radial. L_{s_s} is then the longitudinal length scale and L_{s_u} and L_{s_r} are transverse length scales.

When data are sampled simultaneously as is the case in a computation, the length scales in other directions can also be considered. For instance, the lengths scales based on radial separation can be considered. In this case

$$L_{r_i} = \int_0^\infty \frac{\overline{u_i'(r)+u_i'(r+\triangle r)}}{u_i'^2} d\triangle r \tag{3}$$

Now, when i is r it refers to the longitudinal length scale and $i = s$ or r refers to the transverse length scales.

The mean energy dissipation rate of locally isotropic turbulence is defined as[12]

$$\epsilon = 15\nu \overline{\left(\frac{\partial u_s'}{\partial x_s}\right)^2}, \tag{4}$$

where the derivative of the turbulence intensity can be rewritten in terms of the structure function

$$\overline{\left(\frac{\partial u_s'}{\partial x_s}\right)^2} \approx \frac{S_2^s(x_s)}{x_s^2} \approx \frac{S_2^s(U_s\tau)}{(U_s\tau)^2} \tag{5}$$

with the general Structure function defined as

$$S_n = \overline{(\delta_r \mathbf{u}')^n} = \overline{\left((\mathbf{u}'(\mathbf{x}+\triangle\mathbf{x}) - \mathbf{u}'(\mathbf{x})) \cdot \frac{\triangle\mathbf{x}}{|\mathbf{x}|}\right)^n} \tag{6}$$

such that when the Taylor frozen hypothesis is applied $S_2^s(x_s) = S_2^s(U_1\tau)$. This method will be used to calculate the dissipation rate. The kinematic viscosity is assumed to be a constant, 1.6412 x10^{-4} ft^2/s

IV. Results

A. Mean flow

The mean flow is analyzed first. The total mean values at each radial location at station 1 is shown in Figure 4. HW denotes the hotwire data, LDV denotes the LDV data and LBM denotes the simulation data. It is seen that the axial velocity measured by the hotwire data is a bit higher than that measured with the LDV system and computed by PowerFLOW. The hotwire measured circumferential velocity is a bit lower. These results are consistent with comparisons made between the hotwire data and results from other RANS simulations.[9] The axial and circumferential velocity fields are combined to create the streamwise mean value. By construct, the total mean of the upwash velocity is zero. When the flow is projected into the streamwise direction, the LDV and hotwire measurements agree better. The simulated flow agrees relatively well.

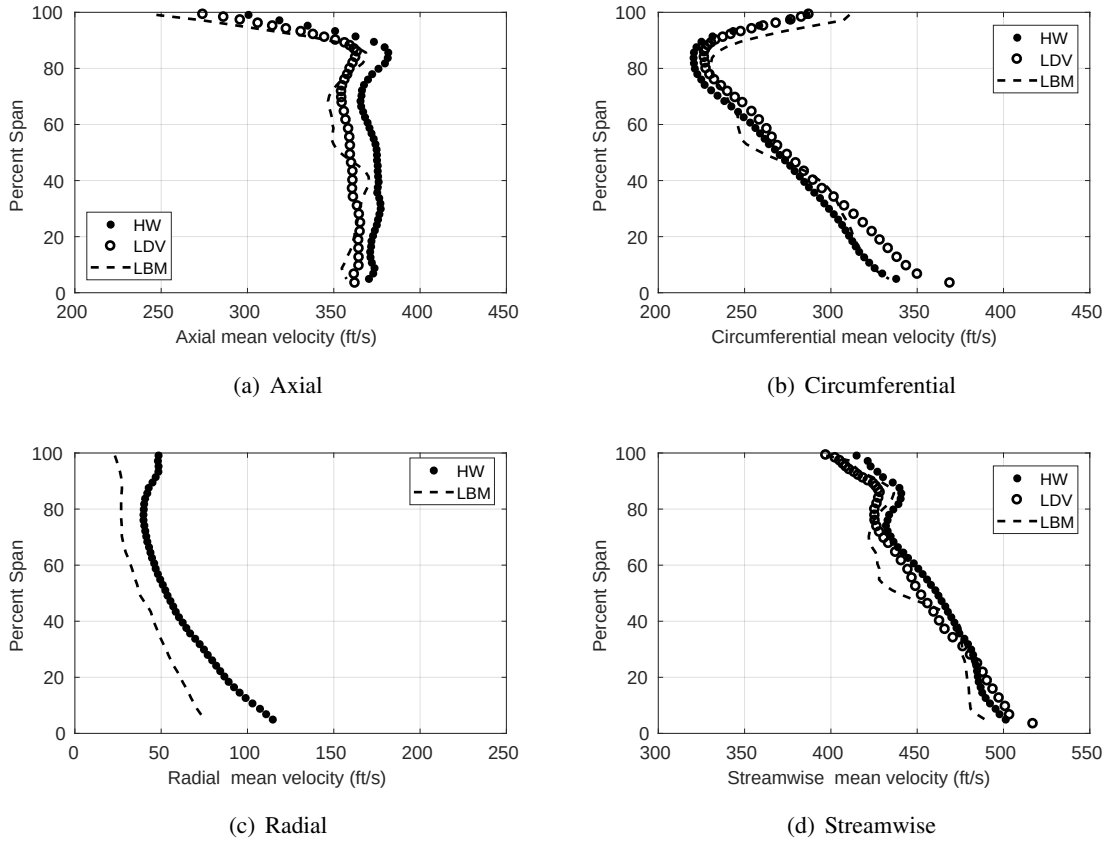

(a) Axial

(b) Circumferential

(c) Radial

(d) Streamwise

Figure 4: Mean flow velocity vs span location at station 1.

The same flow analysis is performed at station 2 and shown in Figure 5. The agreement between the computed values and the measured values is similar at station 2. For the computation, the data has been extracted just ahead of the vane as the actual station 2 location coincides with the leading edge of the vane. Although, the measurements were taken for the low-noise, swept, vane (with a straight leading edge), the flow is shown here to be very similar for the baseline vane.

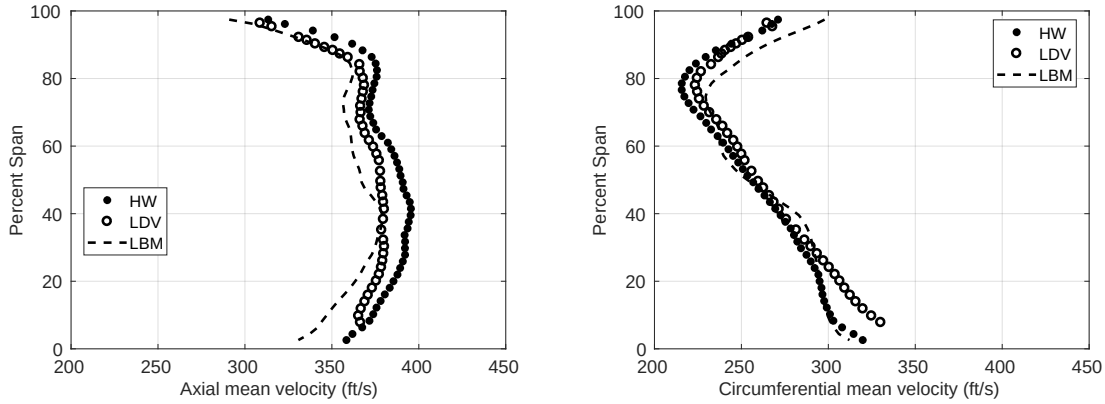

(a) Axial

(b) Circumferential

(c) Radial

(d) Streamwise

Figure 5: Mean flow velocity vs span location at station 2.

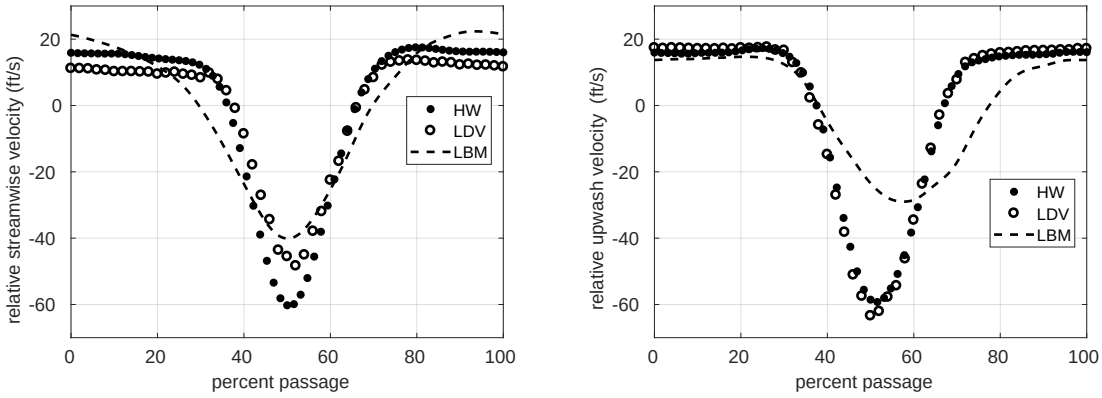

(a) Streamwise

(b) Upwash

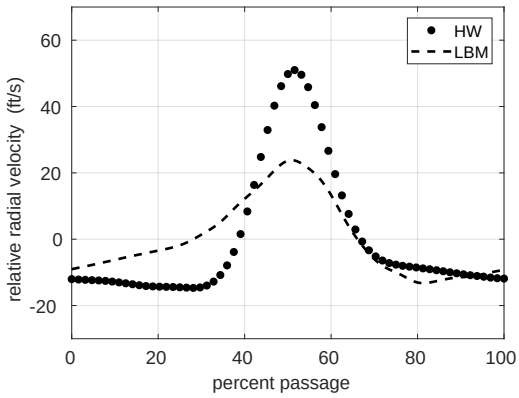

(c) Radial

Figure 6: Midspan average passage velocity components at station 1.

Figure 6 shows the average passage streamwise, upwash, and radial velocity at the 50% span location of measurement station 1. Only two flow components were obtained with the LDV system, so only the hotwire and computational data are compared in the radial direction. The velocity is given in a relative sense in that the relevant total mean has been subtracted from each velocity component. In the figure, 100 revolutions are used to obtain the hotwire values. Figure 7 shows the extremely slight difference when only 10 revolutions are used in the hotwire analysis. This indicates that for mean flow analysis, 10 revolutions is more than enough. However, the comparison indicates that the computation has too much diffusion as the wake depth is too shallow and width is too large. The underprediction of the radial mean value at the midspan shown apparent in Figure 6c as well as the similarity between the average streamwise value from the computation and the LDV data at the midspan are both reflected in Figure 4. Figure 8 shows a similar flow trend at station 2.

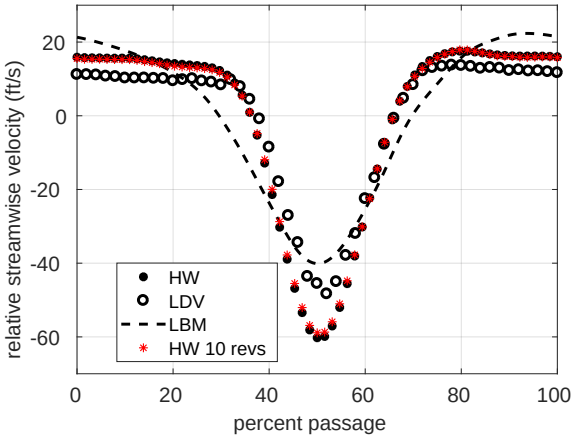

Figure 7: Midspan average passage velocity components at station 1. Comparison between hotwire analysis performed with 100 revolutions and 10 revolutions.

B. Turbulence intensity

The hotwire and PowerFLOW data are processed identically to obtain the RMS, i.e. turbulence intensity, mean and average passage values. Although it is the upwash component of the turbulence intensity that is used in low-order vane response calculation, the turbulence intensity in three directions is given in Figure 9. The closest agreement is seen for the axial component of the turbulence intensity. In this direction, the hotwire and LDV results are almost identical. The computed results agree well. The second component that is provided in the LDV data is understood to be the circumferential velocity. When it is compared to the hotwire and computed values it does not agree well. For the hotwire and computed data, the streamwise, upwash and radial components of the turbulence intensity can be obtained. The higher streamwise values and slightly lower upwash values for the computed results when compared to the experimental values can be attributed to differences in the flow angle used to resolve these flow directions. Figure 4 indicates that especially near the 50% span location, there is a difference between the flow angle provided by the computations and the hotwire mean flow values.

It was shown previously[5] that $\overline{u_s'^2} \approx \overline{u_u'^2} \approx \overline{u_r'^2}$ and that the cross correlations are approximately 0, with the approximates becoming closer to equalities further downstream. This indicates the turbulence is fairly isotropic with the largest deviations from isotropy occurring near the outer endwall. This is best seen when viewing the radial distribution of the mean RMS values as in Figure 10.

For the low-order vane response calculations, the averaged turbulence intensity value at each spanwise location is of interest. Figure 10 provides this data at both stations. The turbulence intensity is smaller at the second station which results from the decay of the turbulence as the wake evolves. The overall agreement of the turbulence intensity is quite good, even at station 2, where the mean flow is highly affected by the potential field of the vane. This indicates that the turbulence is not influence by the potential effect.

The turbulent kinetic energy (k) can also be investigated. It is of interest to obtain this value in order to compare it to the value of k from the subgrid scale model used in the PowerFLOW code. One finds that the k in the subgrid scale model is quite small compared to the computed k from the turbulent velocity.

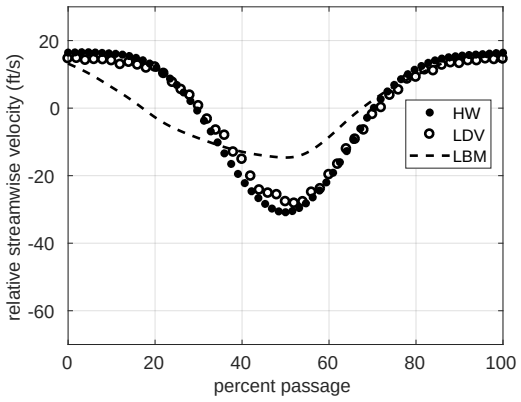

(a) Streamwise

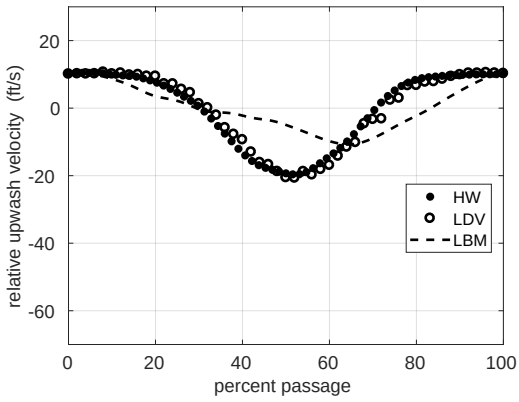

(b) Upwash

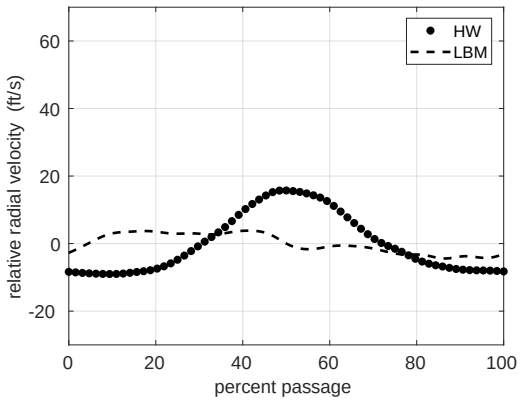

(c) Radial

Figure 8: Midspan average passage velocity components at station 2.

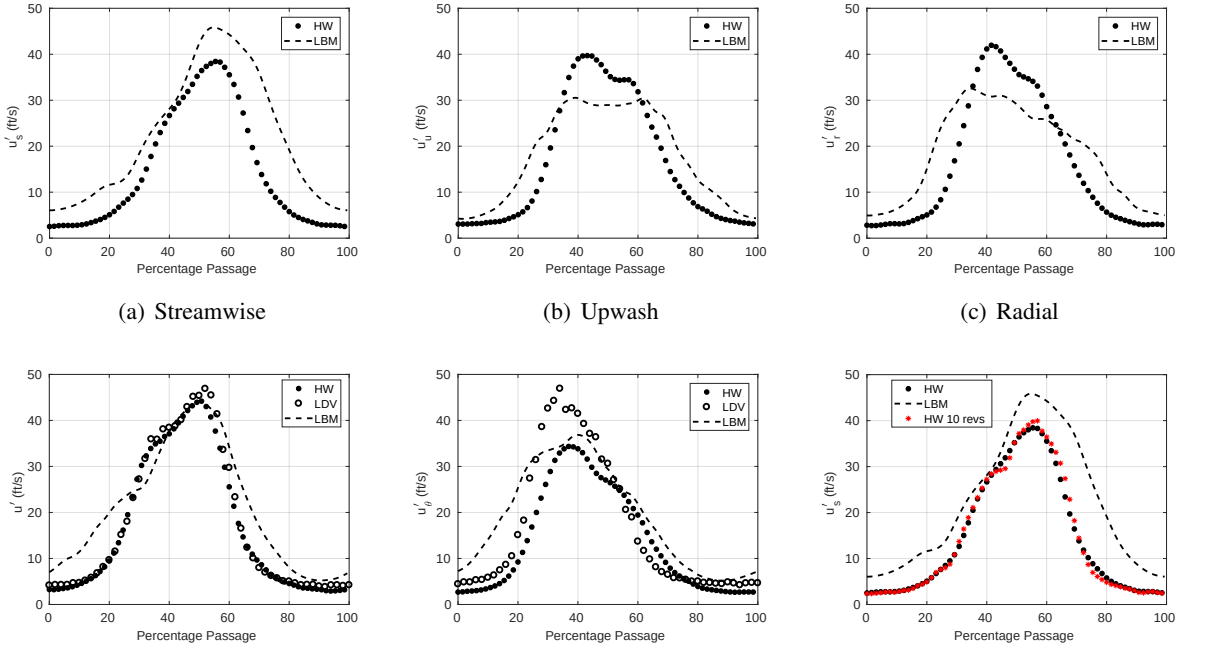

(a) Streamwise (b) Upwash (c) Radial

(d) Axial (e) Circumferential (f) Streamwise, different number of revs

Figure 9: Midspan average passage turbulence intensity at station 1.

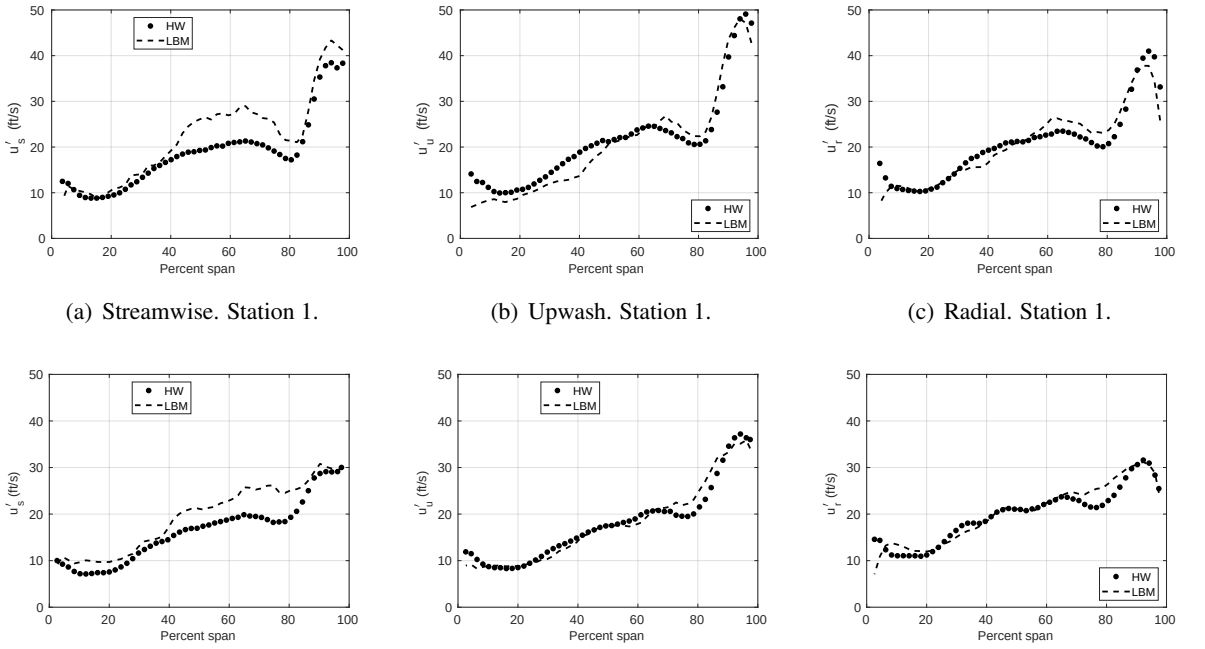

(a) Streamwise. Station 1. (b) Upwash. Station 1. (c) Radial. Station 1.

(d) Streamwise. Station 2. (e) Upwash. Station 2. (f) Radial. Station 2.

Figure 10: Circumferentially averaged turbulence intensity vs radial location at stations 1 and 2.

C. Turbulence length scale

The length scales computed using Eq. (2) are shown in Figure 11. The integration has been performed from 0 to the first zero crossing of the integrand. It is noted that the computed axial flow is mainly responsible for the large excursions in the longitudinal length scale. The transverse length scales computed from the simulation data are 1.5 times larger than those computed from the hotwire data. Investigation of the correlation at the midspan indicates that indeed the length scale predicted by the computation is large.

Figure 12 shows the integrand of Eq. (2) at the midspan. The correlation of the simulated data does not go to zero until 60 μs while the correlation of the hotwire data crosses zero at 20 μs. In addition the slope of the correlation curve is smaller for the simulated data. Both of these factors lead to the much larger length scale. It has been verified as shown in Figure 12 that this is not a function of the number of revolutions used to obtain the turbulent statistics. It has also been verified that this is not an outcome of differences in the meanflow, indeed the streamwise mean velocity U_s that appears in Eq. (2) is quite similar for the hotwire and simulation data as shown in Fig. 4. Finally, it has been verified that the large difference is not an outcome of projecting the original velocity data into the streamwise direction, as the correlations that can be computed using the axial velocity shows the same large discrepancy.

As shown in Casalino et al.,[7] a trip is used in the computation to trigger the turbulent transition on the rotor blades and thus recover the level of turbulent fluctuations through the whole span. It has been shown that the trip is not necessary to match the sideline operating condition, and a finer mesh resolution near the rotor blades results in a more accurate prediction of the turbulent wake development downstream of the rotor.[13] It can be argued that the presence of the trip allows recovering the fluctuation levels, but it affects the turbulent scales by promoting the generation of larger scale fluctuations. Further analyses will be conducted in the future to verify this hypothesis.

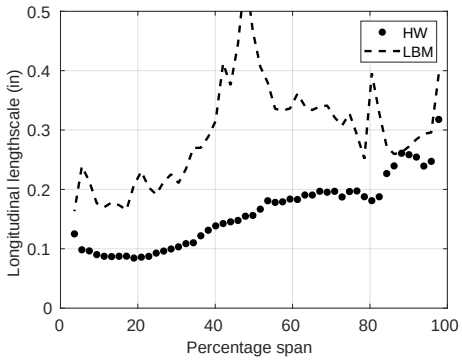

(a) Streamwise.

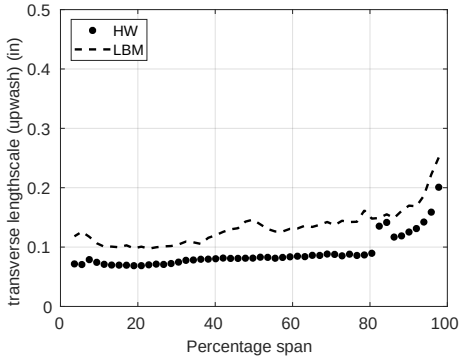

(b) Upwash.

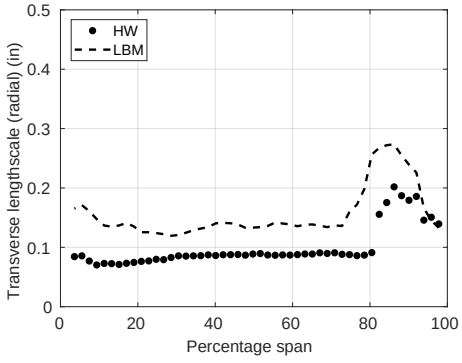

(c) Radial.

Figure 11: Radial distribution of turbulence length scales at station 1.

Similarly, at the second station, the length scales based on the hotwire data and the simulation data are off by a factor of 1.5 and again there are larger excursions in the longitudinal (streamwise) length scale. The length scales at the second station are shown in Figure 13 with the simulation based values divided by 1.5 to highlight this scale difference.

The other length scale that appears in the low-order broadband vane response calculation is the radial length scale of the upwash velocity. This quantity is related to the transverse correlation in the radial direction. Because the simulated data are obtained simultaneously, one can use the data at neighboring radial points to form the transverse length scale in the radial direction via Eq. (3). However, all of the radial data are used to obtain a single length scale. Therefore one does not have the ability to probe the radial length scale as a function of radial position. The values are given in Table 1. The length scales can be compared to those found in the streamwise direction. The pertinent streamwise values are also given in the table. Finally, one can use the circumferential (or passage) direction to compute the length scales. At every radial location, the axial, circumferential and radial turbulent velocities can be used to obtain length scales where the separation is taken to be in the circumferential direction. The relation between the transverse and longitudinal length scales when utilizing the circumferential direction is not as close to the factor of two seen in the other directions.

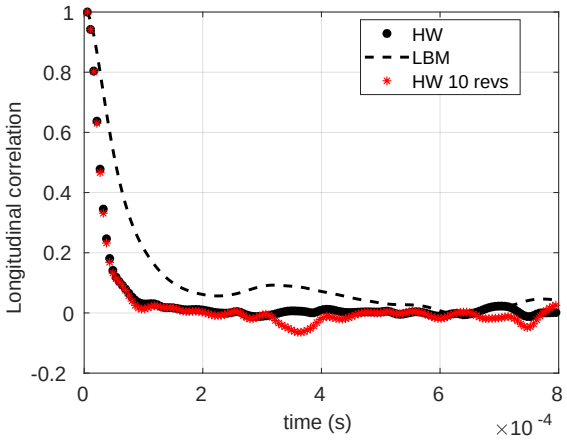

Figure 12: Normalized streamwise turbulent velocity correlation (integrand of Eq. (2) at midspan. The hotwire data was analyzed with both 100 revolutions and 10 revolutions.

Similar length scale comparisons can be made at station 2. The length scales are larger farther downstream as the turbulence in the wake evolves. Again there is reasonable agreement between the longitudinal and transverse scales computed in the stream and radial directions. The circumferential length scales have not yet been processed at station 2. The relation between the longitudinal and the transverse length scales is a factor of about 2. This is what is expected for isotropic turbulence. It may be concluded that if one requires a radial distribution of the transverse radial length scale (as is the case for the low-order model), it is reasonable to assume that utilization of transverse length scale computed in the streamwise direction (which can be found as a function of radius) is a plausible approximation.

Table 1: length scale values computed from simulation data at station 1.

Type		(in)		(in)		(in)
Longitudinal	L_{r_r}	0.3	L_{s_s}	0.29	L_{c_c}	0.21
Transverse	L_{r_s}	0.18	L_{s_u}	0.13	L_{c_a}	0.16
Transverse	L_{r_u}	0.21	L_{s_r}	0.16	L_{c_r}	0.18

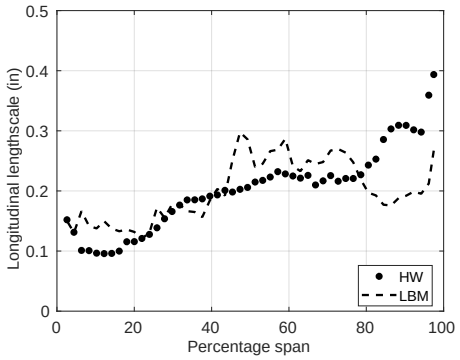

(a) Streamwise.

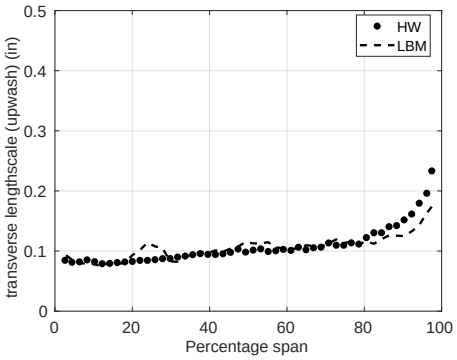

(b) Upwash.

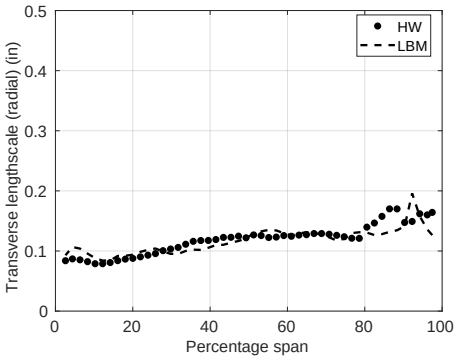

(c) Radial.

Figure 13: Radial distribution of turbulence length scales at station 2. Simulation based values have been divided by 1.5.

Table 2: length scale values computed from simulation data at station 2.

Type		(in)		(in)
Longitudinal	L_{r_r}	0.37	L_{s_s}	0.33
Transverse	L_{r_s}	0.20	L_{s_u}	0.16
Transverse	L_{r_u}	0.17	L_{s_r}	0.18

D. Turbulent dissipation

The structure function at midspan computed from the hotwire data and the simulation data is shown in Figure 14. The right hand side of Eq. (5) is also shown in Figure 14. It is clear from Fig. 14(b) that the time step at which the hotwire data were acquired is not small enough to provide the flattening of the curve at small time. However, it is close to its final value and as such the smallest time step shown in the figure for both the hotwire and the simulation based values is used to obtain the radial distribution of the mean turbulent dissipation rate. The result is shown in Figure 15. From previous comparisons, the value of ϵ obtained from

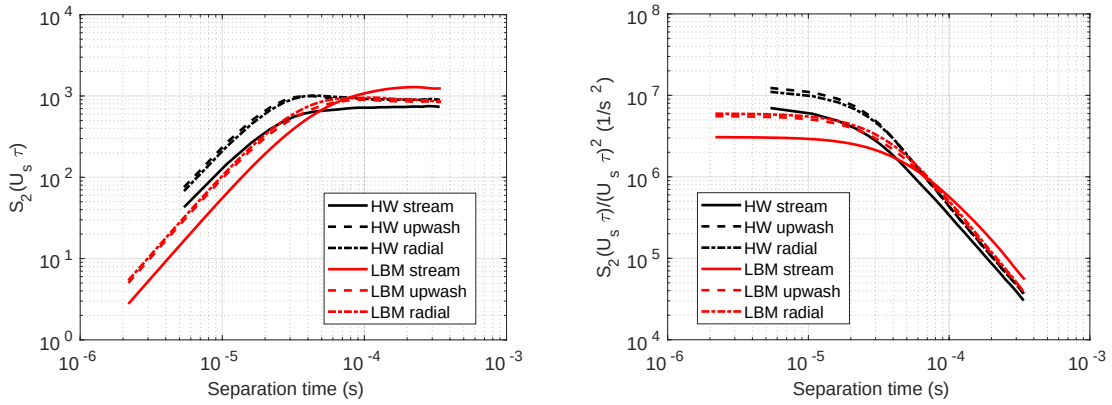

(a) Eq. (6) (b) Eq. (5)

Figure 14: 2nd order structure function and the structure function divided by $(U_s\tau)^2$ at midspan station 1.

the simulation is quite similar to that found from the hotwire data. When RANS simulation ϵ values were obtained, it was shown that they were two orders of magnitude larger than the hotwire derived values. It is left for a future investigation to compare the dissipation rate used in the subgrid scale model used in the PowerFLOW code to the ϵ found here from the turbulent velocity.

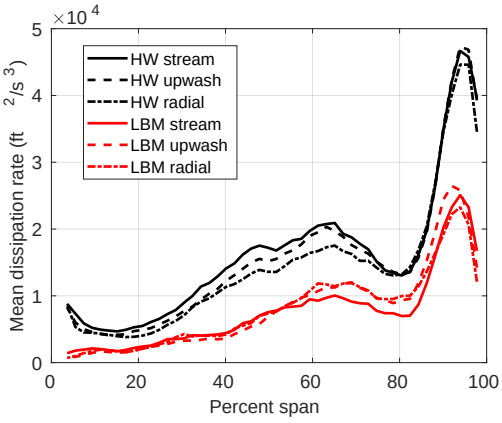

Figure 15: Radial distribution of mean turbulent dissipation rate from Eq. (4).

E. Impact of gap flow differences on broadband noise prediction

The low-order turbofan broadband prediction method described in Ref. [9] is used with input generated from the hotwire and the PowerFLOW simulations. In particular, the quantities that are utilized are the radial distribution of axial and circumferential mean flow, the radial distribution of the mean upwash turbulence intensity, and the radial distributions of the streamwise longitudinal length scale and the radial transverse (upwash) length scale. The radial transverse length scale has been previously implemented in two ways. It has been set to 1/2 the longitudinal streamwise length scale as justified in Section C. It has also been determined based on the method introduced by Posson et al.[14]

$$L_{r_u} = \frac{3\pi L_{s_s}}{2\sqrt{1+(k_s L_{s_s})^2}} \frac{(k_s L_{s_s})^2}{1+3(k_s L_{s_s})^2} \tag{7}$$

The power spectrum at the exhaust exit is used as the acoustic outcome comparison. Figure 16 shows the values provided by NASA as part of the fan broadband benchmark distribution compared to previously computed predictions using input based on the hotwire data (HW). The figures also show the predictions obtained using input data based on the PowerFLOW results. The mean and turbulent flow quantities at station 2 have been used (LBM). The factor of 1.5 on the streamwise longitudinal length scale is shown to be the main source of the difference in the predictions. An input set which utilized the mean flow and RMS values from PowerFLOW but the length scale from the hotwire data (LBM with HW L_s) are very similar to the HW results. This differences will be studied more carefully in the future.

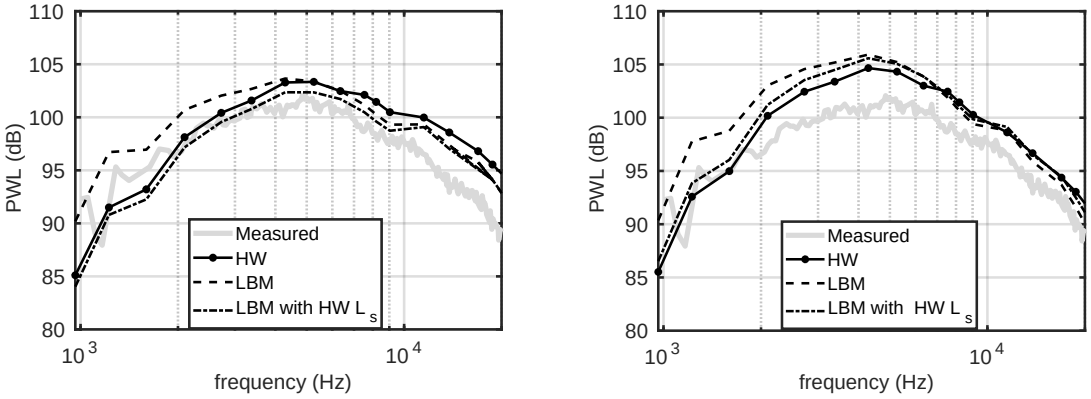

(a) $L_{r_u} = 0.5 L_{s_s}$ (b) Eq. (7)

Figure 16: SDT baseline vane case at approach speed. Results from low-order fan broadband prediction with input based on HW data, PowerFLOW data and a combination. Mid-chord stagger has been used in the low-order model. The radial distribution of the transverse radial length scale is computed two ways.

V. Conclusions and future work

The flow field computed using PowerFLOW for a slightly modified SDT baseline vane at the approach fan speed has been quantitatively compared to measurements in the interstage region. The mean wake at the mid gap is already more diffuse than seen experimentally. This would impact the tonal noise which

has not been considered in this study. The turbulence intensity is well predicted at both the mid gap and near the vane leading edge. The turbulent length scale is higher in the computation by a factor of about 1.5. The source of this discrepancy is not clear although the higher wake diffusion can play a role as well as the utilization of a trip on the rotor in the PowerFLOW calculation. The turbulent dissipation rate is slightly lower than that calculated from the hotwire data, but is on the right order as compared to the ϵ found previously using RANS CFD which is two orders of magnitude higher.

When the PowerFLOW data are used as input to a low-order vane response method for predicting the broadband noise in the exhaust duct, it is shown that the overprediction of the streamwise longitudinal length scale has the largest affect on the noise predictions. It is of interest to consider why this effect was not prominent when the acoustics were computed directly from the PowerFLOW code previously. Future comparisons of the vane response computed directly in the PowerFLOW code and from the low-order vane response method may give insight into this discrepancy.

The relation of the subgrid k and ϵ to the computed values is still left to be considered. Also, the radial distributions shown throughout this paper were all obtained by considering the results at a single circumferential location. One has access to all circumferential locations across a passage, and it has been noted that if a different location is selected, the radial distribution is altered slightly. More analysis needs to be done to understand the implication of this finding. Further assessment of the circumferential length scales is required in order to understand why the relationship between the longitudinal and tranverse scales in this direction is not the same as in the other directions.

Additional studies of interest that may be possible in the future include the comparison of PowerFLOW interstage flow data at higher fan speeds with the LDV data as well as RANS CFD data that have been analyzed in the past. It is also of interest to consider the different vane geometries and to further study the potential field's impact on both the mean and turbulent flow. A method to include analysis of the flow field on axial slices closer to the fan trailing edge would allow for a full wake evolution study that could include the evolution of both the mean and turbulent flow quantities.

VI. Acknowledgments

The past efforts of BU graduate alum Jeremy Maunus, Professor Emeritus Victor Yakhot, and past BU RCS staff member Douglas Sondak are recognized for providing the quantitative assessment method for the interstage turbulent flow. The authors also acknowledge that the data analysis and low-order fan broadband calculations reported in this paper were performed on the Shared Computing Cluster which is administered by Boston University's Research Computing Services. The SDT results belong to the RC1 portfolio of benchmark problems designed to assess the state of the art in fan broadband noise prediction. Further information may be found at http://www.oai.org/aeroacoustics/FBNWorkshop. Ed Envia is acknowledged for his work compiling and distributing the fan broadband workshop geometry and data.

References

[1]Heidelberg, L. J., "Fan Noise Source Diagnostic Test-Tone Modal Structure Results," *AIAA Paper No. 2002-2428*, 2002, 8th AIAA/CEAS Aeroacoustics Conference.

[2]Woodward, R. P., "Fan Noise Source Diagnostic Test-Farfield Acoustic Results," *AIAA Paper No. 2002-2427*, 2002, pp. 1–12., doi : 10.2514/6.2002-2427.

[3]Envia, E., "Fan Noise Source Diagnostic Test-Vane Unsteady Pressure Results." *AIAA Paper No. 2002-2430*, 2002, 8th AIAA/CEAS Aeroacoustics Conference.

[4]Envia, E., c. Hughes, Podboy, G., and Woodward, R., "Fan Noise Souce Diagnostic Test Completed and Documented," Tech. Rep. TM-2005-0214860, NASA, 2003.

[5]Maunus, J., Grace, S. M., Sondak, D. L., and Yakhot, V., "Characteristics of Turbulence in a Turbofan Stage," *Journal of Turbomachinery*, Vol. 135, No. 2, March 2013, pp. 021024–1–10.

[6]Leonard, T., Sanjose, M., and Moreau, S., "Large Eddy Simulation of a scale-model turbofan for fan noise source diagnostic," *AIAA Paper No. 2016-3000*, 2016, pp. 1–24.

[7]Casalino, D., Hazir, A., and Mann, A., "Turbofan Broadband Noise Prediction using the Lattice Boltzmann Method," *AIAA Journal*, Vol. 56, No. 2, 2018.

[8]Maunus, J., Grace, S. M., and Sondak, D. L., "Effect of Rotor Wake Structure on Fan Interaction Noise," *AIAA Journal*, Vol. 50, No. 4, April 2012, pp. 818–831.

[9]Grace, S., "Fan Broadband Interaction Noise Modeling Using a Low-Order Method," *Journal of Sound and Vibration*, Vol. 346, 2015, pp. 402–423.

[10]Podboy, G. G., Krupar, M. J., Helland, S. M., and Hughes, C., "Steady and Unsteady Flow Field Measurements Within a NASA 22-Inch Fan Model," Tech. Rep. TM-2003-212329, NASA, 2003.

[11]Casalino, D., Avallone, F., Gonzalez-Martino, I., and Ragni, D., "Aeroacoustic study of a wavy stator leading edge in a realistic fan/OGV stage," *ISROMAC 2017*, 2017, pp. 1–11.

[12]Kolmogorov, A. N., "The local structure of turbulence in an incompressible viscous fluid for very large Reynolds numbers," *Proc. R. Soc. Lond.*, Vol. 434, 1991, pp. 9–13.

[13]Gonzalez-Martino, I. and Casalino, D., "Fan Tonal and Broadband Noise Simulations at Transonic Operating Conditions Using Lattice-Boltzmann Methods," *AIAA Paper No.*, 2018.

[14]Posson, H., Moreau, S., and Roger, M., "Broadband noise prediction of fan outlet guide vane using a cascade response function," *Journal of Sound and Vibration*, Vol. 330, 2011, pp. 6153–6183.